Chemical Geology 590 (2022) 120705

Contents lists available at ScienceDirect

Chemical Geology

journal homepage: www.elsevier.com/locate/chemgeo

Uranium isotope cycling on the highly productive Peruvian margin

S. Bruggmann [a,b,*], G.J. Gilleaudeau [c,d], S.J. Romaniello [c], S. Severmann [e], D.E. Canfield [f], A. D. Anbar [c], F. Scholz [g], R. Frei [a]

[a] Department of Geoscience and Natural Resource Management, Geology Section, University of Copenhagen, Øster Voldgade 10, DK-1350 Copenhagen K, Denmark
[b] Department of Earth Sciences, Vrije Universiteit Amsterdam, De Boelelaan 1085, 1081HV Amsterdam, the Netherlands
[c] School of Earth and Space Exploration, Arizona State University, Tempe, AZ 85287, United States
[d] Department of Atmospheric, Oceanic, and Earth Sciences, George Mason University, Fairfax, Virginia 22030, United States
[e] Department of Marine and Coastal Sciences, Rutgers University, 71 Dudley Rd, New Brunswick, NJ 08901, United States
[f] Nordcee, Department of Biology, University of Southern Denmark, Odense, Denmark
[g] GEOMAR Helmholtz Centre for Ocean Research Kiel, Wischhofstraße 1-3, 24148 Kiel, Germany

ARTICLE INFO

Editor: E.B Michael

Keywords:
Redox proxy
Productivity
Anoxic
Non-euxinic
Sequential extraction

ABSTRACT

Uranium isotopes ($\delta^{238}U$ values) in ancient sedimentary rocks (shales, carbonate rocks) are widely used as a tool to reconstruct paleo-redox conditions, but the behaviour of U isotopes under modern non-sulfidic anoxic vs. oxic conditions remains poorly constrained. We present U concentration and isotope data for modern sediments from the Peruvian margin, a highly productive open ocean environment with a range of redox conditions. To investigate U in different host fractions of the sediment (reactive, silicate, and HNO_3-soluble fraction), we conducted a series of sequential extractions. Detrital-corrected authigenic U isotope compositions ($\delta^{238}U_{auth}$) in sediments deposited beneath an oxic water column show little deviation from the dissolved seawater U source, while anoxically deposited sediments have $\delta^{238}U_{auth}$ values that are up to 0.4‰ heavier compared to seawater $\delta^{238}U$. Under anoxic, non-euxinic conditions, the U isotope offset between sediment and seawater is larger compared with oxic, but significantly smaller when compared with euxinic conditions from the literature. The results from sequential extractions show that the reactive sediment fraction records more pronounced differences in $\delta^{238}U_{reactive}$ than $\delta^{238}U_{auth}$ values depending on the oxidation state of the overlying water column. Furthermore, we found a strong correlation between total organic carbon (TOC) and both U concentrations (U_{auth}) and $\delta^{238}U_{auth}$ values ($R^2 = 0.70$ and 0.94, respectively) at the persistently anoxic site that we examined. These correlations can be caused by several processes including U isotope fractionation during microbially-mediated U reduction at the sediment-water interface (diffusive U input), during sorption onto and/or incorporation into organic matter in the water column (particulate U input) and diagenetic redistribution of U, or a combination of these processes. Our data show that several factors can influence $\delta^{238}U$ values including oxidation state of U, the presence or absence of hydrogen sulfide and organic matter. These findings add new constraints to the degree of U isotope fractionation associated with U incorporation into sediments in different low-oxygen environments, thus aiding in interpretation of ancient paleo-redox conditions from U isotope data.

1. Introduction

The oceans underwent substantial changes in their redox state from the Archean Eon to the present (e.g. Diamond and Lyons, 2018), and they are bound to change in the future (e.g., deoxygenation; Keeling et al., 2010; Schmidtko et al., 2017). Reconstructing the extent of ocean anoxia in the past will reveal important information for future predictions. Trace metals such as Mo, V, Cr, and U are powerful tools to record redox changes in marine environments, because their solubility decreases under reducing conditions. However, reducing conditions are not only controlled by dissolved oxygen in seawater, but are also coupled to the rate of organic carbon (C_{org}) rain to and burial in the sediment, processes that can be mutually connected. It is therefore essential to investigate the full range of parameters that can affect such redox-sensitive trace metals.

Hexavalent U in oxic seawater occurs as the stable uranyl carbonate

* Corresponding author.
E-mail addresses: s.bruggmann@vu.nl (S. Bruggmann), ggilleau@gmu.edu (G.J. Gilleaudeau), stephen.romaniell@asu.edu (S.J. Romaniello), silke@marine.rutgers.edu (S. Severmann), dec@biology.sdu.dk (D.E. Canfield), anbar@asu.edu (A.D. Anbar), fscholz@geomar.de (F. Scholz), robertf@ign.ku.dk (R. Frei).

https://doi.org/10.1016/j.chemgeo.2021.120705
Received 2 September 2021; Received in revised form 22 December 2021; Accepted 27 December 2021
Available online 31 December 2021

ion (UO_2-CO_3), or as Ca/Mg-UO_2-CO_3 complexes, at concentrations between 13 and 14 nmol kg^{-1} (Ku et al., 1977; Langmuir, 1978; Endrizzi and Rao, 2014). It behaves conservatively with a long residence time of around 200,000 to 400,000 years (Ku et al., 1977). The major source for U in seawater is riverine input, where U is mobilised from the continental crust during oxidative weathering, and soluble U(VI) is transported to the oceans (Dunk et al., 2002). Anoxic sediments are the main sink for U. Other sinks, such as biogenic carbonates, as well as weathering of basalts at mid-ocean ridges, also play a role (Dunk et al., 2002). Uranium can also be sequestered in sediments as carbonate fluorapatite (CFA), the initial mineral phase of phosphorites (Arning et al., 2009). Under suboxic or anoxic conditions in the sediments, U is removed from porewater via reduction to U(IV) and subsequently replenished by diffusion across the sediment-water interface (e.g. Klinkhammer and Palmer, 1991; Weyer et al., 2008). Reduction of U can take place abiotically or can be mediated by sulfate or Fe reducing bacteria or other microorganisms (Lovely et al., 1991; Rademacher et al., 2006; Basu et al., 2014; Stirling et al., 2015; Stylo et al., 2015; Basu et al., 2020). After reduction to U(IV), U precipitates inorganically as uraninite, UO_2, but can also be present as non-crystalline solid phase as observed for lacustrine environments (Barnes and Cochran, 1990; Klinkhammer and Palmer, 1991; Stetten et al., 2018). In contrast to Mo, U shows less affinity for shuttling to the sediment with Fe and Mn (oxyhydr)oxides (Algeo and Tribovillard, 2009; Scholz et al., 2017). Instead, incorporation into organic particles has been recognised as a mechanism for U delivery to the sediment, especially in high productivity environments such as the Peruvian margin (Anderson et al., 1989a; McManus et al., 2006; Zheng et al., 2002a).

In the water column, U uptake by organisms or sorption onto their surfaces in the surface waters allows transport of particulate non-lithogenic U (PNU) to the sediment (Anderson et al., 1989b). Diffusive accumulation of U at the sediment-water interface and input of U with particulate organic matter can take place in the same setting and are difficult to distinguish. The accumulation of U in sediments can be elevated under reducing conditions (e.g. Black Sea), but also where the C_{org} rain and burial rates are high (e.g. Peruvian margin; Zheng et al., 2002b; McManus et al., 2005). Under oxic conditions, PNU is near-quantitively remobilised before burial (Zheng et al., 2002a). In contrast, under anoxic conditions, U can be preserved and contribute up to 70% of the total authigenic U in sediments. Uranium transport to the sediment can be linked with sinking organic matter in a range of marine environments. Sedimentary U concentrations are therefore being used as a proxy for surface ocean productivity or C_{org} burial rate (e.g. Anderson et al., 1989b; Kumar et al., 1995; Chase et al., 2001; Zheng et al., 2002b; McManus et al., 2006). Other studies, however, have suggested that bottom water oxygen is the primary control of authigenic U accumulation (Francois et al., 1993; Hayes et al., 2014; Abshire et al., 2020).

While U concentrations in sediments have been widely accepted as both a redox and productivity proxy, changes in stable U isotope ratios ($^{238}U/^{235}U$, expressed as $\delta^{238}U$) are mostly interpreted to reflect redox conditions (reviewed by Lau et al., 2019). The most abundant isotopes of U are the primordial ^{238}U and ^{235}U isotopes, with half-lives of 4.5 and 0.7 billion years, respectively. Even though these two isotopes are not stable, given their long half-lives for decay, variations of $^{238}U/^{235}U$ are largely the result of chemical reactions rather than radioactive decay (Weyer et al., 2008). The daughter isotope of ^{238}U, ^{234}U, has a half-life of 248,000 years. The ratio of $^{234}U/^{238}U$ ($\delta^{234}U$) shows large variations caused by alpha recoil, whereby ^{234}U is preferentially expelled from damaged crystal lattices (Kigoshi, 1971). For example, during weathering ^{234}U is preferentially released from the solid to the dissolved phase, eventually leading to a $\delta^{234}U$ value of seawater (147‰), which is higher than secular equilibrium (Chen et al., 1986; Henderson, 2002; Andersen et al., 2010). The $\delta^{234}U$ value of sediments can be used to estimate detrital and authigenic components of the sediment, with seawater-like $\delta^{234}U$ values indicating authigenic U as the dominant component (Andersen et al., 2010; Andersen et al., 2014). Variations of $^{238}U/^{235}U$ are induced by nuclear volume isotope fractionation, whereby the heavy ^{238}U isotope is enriched in the reduced U(IV) species (Bigeleisen, 1996; Fujii et al., 2006; Schauble, 2007). The $\delta^{238}U$ composition of seawater is -0.39 ± 0.02‰ (2SD) and is thought to have been invariant over the past 600,000 years (Andersen et al., 2014; Tissot and Dauphas, 2015). Primary abiotic and biogenic Ca carbonates have been shown to incorporate seawater dissolved U with only minor isotope fractionation (0 to 0.1‰), while modern marine carbonate sediments documented $\delta^{238}U$ values ≈0.3‰ higher than modern seawater due to pore water U(VI) reductions during diagenesis (Stirling et al., 2007; Weyer et al., 2008; Romaniello et al., 2013; Chen et al., 2016; Chen et al., 2018a; Chen et al., 2018b). In contrast, U isotope fractionation up to 0.8‰ ($\Delta^{238}U_{sediment\text{-}seawater}$) is thought to be caused by redox changes occurring during U reduction in porewater prior to accumulation in the sediment (e.g. Weyer et al., 2008). In agreement with the nuclear volume effect (Bigeleisen, 1996; Schauble, 2007), the highest $\delta^{238}U$ values are found in reducing sediments (Weyer et al., 2008). Incorporation of U into primary Ca carbonates does not involve U redox changes and thus, isotope fractionation is minimal under most circumstances (Romaniello et al., 2013; Chen et al., 2016). Uranium sorption onto Fe- or Mn-crusts favours lighter U isotopes, leading to lower $\delta^{238}U$ values in the crusts relative to the seawater source (Brennecka et al., 2011; Goto et al., 2014; Wang et al., 2016). Ranges of U isotope fractionation factors in microbial reduction experiments are large ($\Delta^{238}U_{U(VI)\text{-}U(IV)}$ of up to 1‰) and confirm results from reducing sediments (Basu et al., 2014; Stirling et al., 2015; Stylo et al., 2015). Additionally, U reduction associated with organic matter in surface seawater (sorption on or uptake into organics) induces significant isotope fractionation (Brennecka et al., 2011; Basu et al., 2014; Holmden et al., 2015; Stirling et al., 2015; Stylo et al., 2015; Basu et al., 2020). For example, the U isotope offset $\Delta^{238}U_{plankton\text{-}seawater}$ resulted in −0.79‰ (Holmden et al., 2015). Sorption of U onto particle surfaces can induce both positive and negative U isotope fractionation (e.g. Rademacher et al., 2006; Brennecka et al., 2011; Basu et al., 2014; Basu et al., 2020). Although the processes fractionating U isotopes during sorption on and uptake into organic matter are largely unconstrained, they were recently found to be governed by both the mechanism and the rate of reduction (Basu et al., 2020). A two-step process was suggested, involving 1) sorption of U(VI) on particles or diffusive transport to reduction site and 2) enzymatic reduction to U(IV) (Holmden et al., 2015; Basu et al., 2020).

To accurately interpret the cause of $\delta^{238}U$ variability in ancient sedimentary rocks, studies on $\delta^{238}U$ values in modern marine environments with fine-grained sediments are necessary (Stirling et al., 2007; Weyer et al., 2008; Andersen et al., 2014a; Holmden et al., 2015; Noordmann et al., 2015; Stirling et al., 2015; Hinojosa et al., 2016; Rolison John et al., 2017). Andersen et al. (2014a) present a model where U isotope compositions of modern sediments up to 1.2‰ higher than seawater indicate anoxic or euxinic seawater conditions, whereas values similar to seawater suggest oxic conditions. Under fully sulfidic conditions in porewaters and above, reduction of U diffusing into the porewater is thought to be fast, leading to a large U isotope fractionation of up to 1.2‰ (Andersen et al., 2014a). If the bottom water is oxic and oxygen penetrates the upper porewater, the distance between the sediment-water interface and the zone of U reduction increases (Andersen et al., 2014a). As a result, the measured isotope fractionation decreases (Clark and Johnson, 2008).

Uranium isotope offsets between sediment and seawater are also proposed to be associated with biological processes (possibly in surface water) other than microbial Fe or sulfate reduction (Holmden et al., 2015; Hinojosa et al., 2016; Rolison John et al., 2017; Basu et al., 2020). In Devonian shales, high $\delta^{238}U$ values in the HNO_3-soluble sediment fraction indicate that reduction during sorption or incorporation of U on/into organic particles impacts U isotope compositions (Phan et al., 2018). Lau et al. (2020) highlight the potential of the U isotope system as a productivity proxy. These interpretations are in line with the evident correlation of sedimentary U concentrations with C_{org} delivery to the

sediment (e.g. McManus et al., 2006). However, the relationship between U isotope fractionation and (sinking) organic matter has received little attention for interpretations of $\delta^{238}U$ values in the sedimentary rock record.

This contribution focuses on quantifying U isotope variations in a modern oxic to anoxic, non-euxinic environment with a high C_{org} burial rate. We contribute U isotope data of bulk sediments and sequential extractions from a highly productive open ocean environment (Peruvian margin), along with U concentration data measured on the same sample aliquots. Our data complement previous publications investigating U concentrations and isotope compositions on the Peruvian margin (e.g. Scholz et al., 2011; Cole et al., 2020). These studies are complemented with $\delta^{238}U$ data of sediment samples of up to 28 cm sediment depth, including results from sequential extractions and phosphorites. The insights from our data set are crucial to better understand pathways of U from the water column to the sediment and to reconstruct changes in the global ocean.

2. Methods

2.1. Study area

The Peruvian margin is a well-characterised open marine environment with oxic to anoxic (non-sulfidic) bottom water conditions and high productivity (Table 1, Fig. 1) and is commonly used as a modern analogue for anoxic environments where organic-rich mud sediments are deposited (e.g. Scholz et al., 2017; Scholz, 2018). At the Peruvian margin, upwelling is induced by northwestward blowing winds. This leads to high rates of primary productivity, high export production, and a C_{org} burial rate of 6.8 mmol m^{-2} d^{-1} (mean rate on the total margin (0 to 1000 m depth); Dale et al., 2015). The fine-grained sediments on the Peruvian margin contain up to 20 wt% total organic carbon (TOC), biogenic silica and authigenic phosphate minerals, e.g. carbonate fluorapatite (Krissek et al., 1980; Reimers and Suess, 1983; Froelich et al., 1988; Böning et al., 2004; Gutiérrez et al., 2008).

The core of the oxygen minimum zone (OMZ) becomes anoxic due to the intense degradation of organic material (OM) in the water column (Molina-Cruz, 1977; Brockmann et al., 1980; Gutiérrez et al., 2008; Thamdrup et al., 2012). The water column on the Peruvian margin is not euxinic, contrasting anoxic, euxinic basins such as the notably restricted Black Sea (Anderson et al., 1989a). Our sample set consists of sediment samples from six short (< 50 cm) cores spanning a transect from the oxic shelf through the OMZ to below the OMZ (Fig. 1a). Within the OMZ, the bottom water oxygen is below detection limit in three cores from the shelf to slope (BIGO05, MUC29, MUC19; bottom water oxygen data from Scholz et al., 2011). The stations BIGO05 and MUC29 sporadically experience exposure to low-oxygen bottom water (Levin et al., 2002), but conditions were anoxic when the samples were collected. Below the lower redoxcline, bottom water oxygen increases from 2 to 39.9 μM between cores MUC41, MUC25 and MUC15 (Scholz et al., 2011). Fig. 1b illustrates the OMZ based on oxygen data from GP16, a transect 1°S of our stations (US GEOTRACES; Moffett and German, 2018; Schlitzer et al., 2018). At our study sites, hydrogen sulfide (H_2S) concentrations in the porewaters are insufficient to build up at or above the sediment-water interface most of the time (e.g. Scholz et al., 2011). At the time of sampling, only two stations (MUC19 and MUC29) had H_2S concentrations above detection limit (≈ 2 μM). These increases in H_2S occurred below sediment depths of 10 cm (MUC19) and 20 cm (MUC29), respectively (Scholz et al., 2011). Hence, the majority of the sediment samples investigated here are non-sulfidic and all samples were deposited in a non-euxinic environment. The core MUC41 was only sampled for phosphorites.

Table 1
Locations of the sampling sites with data from Scholz et al., 2011.

Station	Longitude	Latitude	Water depth (m)	BW O_2 (μM)
BIGO05	77°47.7' W	11°00.0' S	85	< LD
MUC29	77°56.6' W	11°00.0' S	145	< LD
MUC19	78°10.0' W	11°00.0' S	319	< LD
MUC41	78°20.9' W	11°00.0' S	510	2
MUC25	78°25.6' W	11°00.0' S	697	12.1
MUC15	78°30.0' W	11°00.0' S	930	39.9

BW = bottom water.

2.2. Sediment sampling

Sediment cores from the Peruvian margin were retrieved using a multi corer (MUC) or obtained from benthic lander deployments (Biogeochemical Observatory, BIGO) in 2008 during the M77–1 and M77–2 cruises of RV Meteor (Scholz et al., 2011). Subsamples (1–5 cm slices) of the sediment cores were taken in an argon-flushed glove bag.

2.3. Uranium concentration and isotope analysis

2.3.1. Uranium separation

To provide a detailed geochemical insight into the composition of the sediments, U concentrations and isotope compositions were analysed on bulk samples as well as on separated fractions (reactive, silicate and organic and pyrite fraction) using a sequential extraction (Huerta-Diaz and Morse, 1990; Bruggmann et al., 2019). These data complement previously published analyses of U concentrations in sediments and porewater on the Peruvian margin (e.g. Scholz et al., 2011).

2.3.1.1. Bulk. A sample size of approximately 20–100 mg was chosen to achieve a total U amount of approximately 500 ng U. Samples were incinerated in ceramic vessels to oxidise organic matter and digested following the standard procedure for mud sediments using concentrated HF and aqua regia (e.g. Bruggmann et al., 2019).

2.3.1.2. Sequential extraction. Sequential extraction was conducted following procedures adapted from Scholz et al. (2007) and Huerta-Diaz and Morse (1990). The following phases were targeted by our sequential extraction scheme:

2.3.1.3. Reactive fraction. Samples were shaken in 15 ml 0.5 M HCl at room temperature for 1 h. The supernatant after centrifugation comprises the sample with amorphous Fe- and Mn-oxyhydroxides, carbonates, hydrous aluminosilicates, and Fe monosulfides.

2.3.1.4. Silicate fraction. Two washing steps with MilliQ (MQ) were conducted after HCl extraction of the reactive fraction and each rinse solution was discarded. These steps were followed by addition of 1 ml concentrated HF. The HF was dried down and another 1 ml concentrated HF was added to the sample to ensure complete dissolution of the silicate fraction. After complete evaporation, the silicate fraction was redissolved in MQ (50 ml) and 0.1 M HCl (10 ml), centrifuged, and decanted. The supernatant of the subsequent washing step (50 ml MQ) was added to the decanted solutions, altogether comprising U associated with clay and silicate minerals.

2.3.1.5. HNO_3-soluble fraction. The residue was treated with 2 ml concentrated HNO_3 and ultrasonicated for 15 min and evaporated to dryness. This fraction contains U associated with organic matter and pyrite.

2.3.1.6. Phosphorites. Phosphorites from MUC41were washed with MQ, 0.1 M HCl and MQ to remove particles prior to crushing with an agate mill (mortar/pestle). Samples were weighed (approximately 30–100 mg) and leached with 0.05 M HCl (shaking table, 1 h) to remove

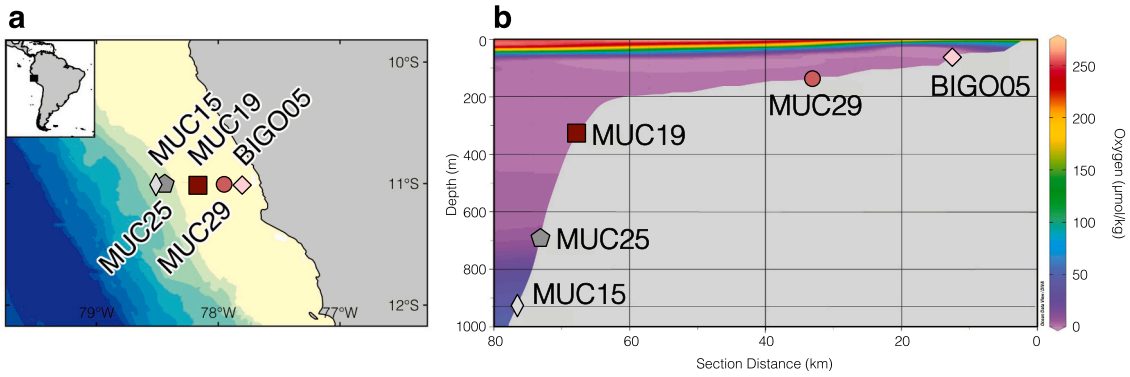

Fig. 1. Map of sampling sites. a) Bathymetry map indicating locations of sampling sites on the Peruvian margin (GEBCO Compilation Group (2020) GEBCO 2020 Grid). b) Oxygen data (CTD) are based on US GEOTRACES cruise GP16, visualised in Ocean Data View (Moffett and German, 2018; Schlitzer et al., 2018).

carbonate. Subsequently, the phosphorite samples were dissolved using aqua regia.

All samples were treated with a mixture of 1 ml concentrated HNO_3 and 100 µl H_2O_2 to remove residual organic material. If samples were not completely dissolved, an additional step using reversed aqua regia as well as another HNO_3:H_2O_2 step (2 ml:0.4 ml, cap and let react overnight) were applied. If necessary, 2.5 ml of 70% perchloric acid was added to the HNO_3:H_2O_2 mixture, capped and cooked at 180 °C for 6–8 h and subsequently evaporated.

2.3.1.7. Concentration analysis. Samples were redissolved in 0.3 M HNO_3 and aliquots (50 µl, diluted to 5 ml) were taken for concentration analysis with inductively-coupled plasma mass spectrometry (ICP-MS), using the iCap-Q ICP-MS Thermo Fisher at Arizona State University (ASU). The precision of U concentrations of repeatedly analysed standard solutions was ±2% ($n = 11$).

2.3.1.8. Chromatographic separation. Prior to chromatographic separation, samples were adequately spiked with a ^{233}U:^{236}U double-spike to reach a spike:sample ratio of ≈ 0.03 (Weyer et al., 2008; Chen et al., 2016), evaporated and re-dissolved in 5 ml 3 N HNO_3. A sample of pre-dissolved rock standard (black shale SDo-1), as well as two CRM145, were processed over the columns along with the samples.

The column chemistry was conducted following Andersen et al. (2004), Romaniello et al. (2013), and Chen et al. (2016). Anion columns (BioRad) were loaded with 0.8 ml UTEVA resin (Eichrom). The resin was pre-cleaned with 4 times 2.5 ml 0.05 M HCl and preconditioned with 3 times 0.8 ml 3 M HNO_3. The sample was then added to the column, and matrix elements were eluted with 5 times 2 ml 3 M HNO_3. Subsequently, 3 times 0.8 ml 10 M HCl were loaded onto the column and Th was eluted using 3 times 0.8 ml of a mixture of 5 M HCl and 0.05 M oxalic acid. To remove the oxalic acid, 3 times 0.8 ml 5 M HCl was added to the column. Finally, U was eluted and collected using 7 ml 0.05 M HCl (1 + 1 + 1 + 2 + 2 ml).

To remove organic residue from the columns, samples were treated with a mixture of concentrated HNO_3 and 30% H_2O_2 (2 ml + 300 µl, respectively), capped and heated for 3–4 h, evaporated and re-dissolved in 2 ml 3 M HNO_3 before repeating the column chemistry for further purification.

2.3.2. Isotope analysis

After the chromatographic separation of U, U isotopes were analysed using a multi-collector ICP-MS (MC-ICP-MS, Thermo Scientific Neptune) at ASU. The samples were re-dissolved in 0.3 M HNO_3 to achieve a U concentration of ≈ 50 ppb and injected into the MC-ICP-MS using an Apex-Q desolvation introduction system. The ion beams of U isotopes (^{233}U, ^{234}U, ^{235}U, ^{236}U, and ^{238}U) were analysed in Faraday cups connected to resistors with 10^{12} or 10^{11} Ω (^{238}U) at a typical ion beam of ≈ 30 V for ^{238}U.

The results are reported as shown in Eqs. 1 and 2 as $\delta^{238}U$ and $\delta^{234}U$ in permille (‰) with the precision indicated as two standard error (± 2SD) of replicate runs. The number of runs is indicated in brackets, duplicates or triplicates of samples are stated as *n*.

$$\delta^{238}U = \left(\frac{\left(^{238}U/^{235}U\right)_{sample}}{\left(^{238}U/^{235}U\right)_{CRM\ 145}} - 1 \right) * 1000 \quad (1)$$

$$\delta^{234}U = \left(\frac{\left(^{234}U/^{238}U\right)_{sample}}{\left(^{234}U/^{238}U\right)_{CRM\ 145}} - 1 \right) * 1000 \quad (2)$$

The certified standard CRM 145 shows a reproducibility of $\delta^{238}U$ and $\delta^{234}U$ values of replicate analysis of ±0.07‰ and ± 3.6‰, respectively (2 SD, n = 11). The average U isotope composition of the Devonian Shale USGS standard reference material SDo-1 was −0.07 ± 0.06‰ (2SD, n = 7), which is within error of published values for this standard (e.g. Abshire et al., 2020).

2.3.3. Corrections for detrital and U

To investigate the influence of marine environmental conditions on U concentrations and isotope compositions in sediments, we calculated the authigenic fraction of U that has interacted with seawater rather than U contained in unreactive terrigenous sediment components. Bulk U concentrations and $\delta^{238}U_{bulk}$ values represent a mixture of all sediment fractions hosting U. Authigenic U concentrations (U_{auth}) and isotope compositions ($\delta^{238}U_{auth}$) were calculated using Al as an indicator of f_{det}, the unreactive detrital (det) sediment fraction (e.g. Tribovillard et al., 2006).

$$U_{auth} = U_{sample} - \left(\left(\frac{U}{Al} \right)_{det} * Al_{sample} \right) \quad (3)$$

Authigenic U isotope compositions were calculated using the detrital correction equation (Eqs. 4 and 5). We used $(U/Al)_{det} = 1.8 * 10^{-5}$ and $\delta^{238}U_{det} = -0.3$‰ to correct for detrital contributions, as the $\delta^{238}U_{det}$ value is thought to be similar to the continental crust (McManus et al., 2006; Weyer et al., 2008; Andersen et al., 2014a).

$$\delta^{238}U_{auth} = \frac{\delta^{238}U_{bulk} - \delta^{238}U_{det} * f_{det}}{1 - f_{det}} \quad (4)$$

$$f_{det} = \frac{Al_{sample} * \left(\frac{U}{Al} \right)_{det}}{U_{sample}} \quad (5)$$

Isotope offsets between seawater and authigenic U in the sediments were calculated using

$$\Delta^{238}U = \delta^{238}U_{auth} - \delta^{238}U_{seawater} \quad (6)$$

with the typical seawater value ($\delta^{238}U_{seawater,\ global} = -0.39‰$; Andersen et al., 2014a

3. Results

3.1. U concentrations

Under oxic conditions below the OMZ, sedimentary U_{auth} concentrations range between 6.05 and 11.55 ppm (Fig. 2a, Table 2), with f_{det} ranging between 0.02 and 0.32. The reactive fractions at the oxic stations contain between 4.84 and 2.94 ppm U (Fig. 3a, Table 3). The HNO_3-soluble fraction contains very little U (as low as 0.06 ppm in BIGO05). The phosphorites contain highly variable U concentrations (6.80 to 73.8 ppm). In the anoxic cores (BIGO05, MUC29, MUC19), U_{auth} concentrations range between 2.34 and 19.46 ppm.

All stations show an increase in U_{auth} with depth from 2.34–9.23 ppm at the surface to 3.66–11.55 ppm at depth. The increase is most pronounced at the most anoxic station MIC19, where concentrations reach a maximum of 19.46 ppm at 4 cm depth. At MUC19, however, concentrations decrease again with depth, reaching a value of 6.39 ppm at 30 cm depth, which is in the same range as the remaining stations.

In the sequentially extracted near-surface samples, the highest U concentrations are found in the reactive fraction of MUC19 (24.29 ppm; Fig. 3a, Table 3), and the reactive fractions of the anoxic stations (BIGO05, MUC29 and MUC19) overall show concentrations of between 1.65 and 24.29 ppm. The concentrations of the reactive fractions compare well with calculated U_{auth} concentrations, for example in MUC19, where the reactive fraction shows a U concentration of 24.29 ppm, compared with a U_{auth} of 19.46 ppm.

3.2. U isotope compositions

The detrital-corrected $\delta^{238}U_{auth}$ values are within error of the bulk $\delta^{238}U$ values (Table 2). Samples from the oxic stations (MUC25 and MUC15) span a tight range of authigenic U isotope compositions from −0.34 to −0.25‰ (Fig. 2b, Table 2). Uranium isotope offsets ($\Delta^{238}U_{auth\text{-}seawater}$) between sediments ($\delta^{238}U_{auth}$) and seawater are around 0.10‰ under oxic conditions (Table 2). Reactive fractions of samples towards the deepest portion of the OMZ (MUC25) and below the OMZ (MUC15) are −0.43‰ and − 0.35‰, respectively. Due to the low contribution of the HNO_3-soluble fraction to the total U, and analytical limitations, HNO_3-soluble fractions were not analysed for U isotope compositions. The $\delta^{238}U$ values of HF extracts typically range around −0.25 ± 0.07‰ (2SD). The phosphorite nodules show the lowest $\delta^{238}U$ values from −0.80‰ to −0.47‰.

Bulk $\delta^{234}U$ values in sediments are lighter than seawater $\delta^{234}U$ values (147‰; e.g. Andersen et al., 2010), showing values of 106‰ or lower in oxic sediments (Fig. 2c). The sequential extractions of sediments deposited under oxic conditions show a large range of $\delta^{234}U$ values between 49‰ and 134‰, with the reactive fraction recording $\delta^{234}U$ values close to seawater. The silicate fraction shows a clear offset from the $\delta^{234}U_{seawater}$ value (BIGO05: 104‰, MUC29: 107‰), except for MUC19. The phosphorite nodules show $\delta^{234}U$ values from −57‰ to 42‰.

Anoxic cores show a range of $\delta^{238}U_{auth}$ values (−0.33 to 0.01‰; Fig. 2b, Table 2), with the highest $\delta^{238}U_{auth}$ value found in a sample from MUC19 at 3.5 cm sediment depth. At this sediment depth, the H_2S concentration is below detection limit. The $\Delta^{238}U_{auth\text{-}seawater}$ values range up to 0.40‰ under anoxic and typically non-sulfidic conditions (Table 2). The reactive fractions of the sequentially extracted sediment samples from the permanent OMZ and the shelf range from −0.20 to −0.04‰ (Fig. 3b). The silicate fraction of the sample from the permanent OMZ (MUC19) is higher compared with other silicate fractions (−0.06‰). Analyses of bulk $\delta^{234}U$ values of Peruvian margin sediments show that all samples from the core of the permanent OMZ (MUC 19) are between 130 and 147‰, very close to seawater (Fig. 2c). The reactive fraction of anoxic samples consistently records seawater-like $\delta^{234}U$ values (147‰). The silicate fraction from the permanent OMZ is higher compared with other silicate fractions (135‰).

4. Discussion

4.1. Comparison of samples from oxic and anoxic stations

At most sites investigated in this study, authigenic U is accumulating, as suggested by the increasing solid U concentrations with depth (Fig. 2a). Authigenic U concentrations in the shallowest stations (BIGO05 and MUC29) are the lowest of the five sites analysed, consistent with fluctuating bottom water oxygen concentrations that can cause U accumulation as well as U remobilisation. At these sites, porewater U (U_{PW}) concentrations increase in the surface sediment, which was attributed to episodes of oxygenation, during which U can be reoxidised and recycled across the benthic boundary (Zheng et al., 2002a, 2002b; Gutiérrez et al., 2008; Scholz et al., 2011). Most sites show U_{auth}

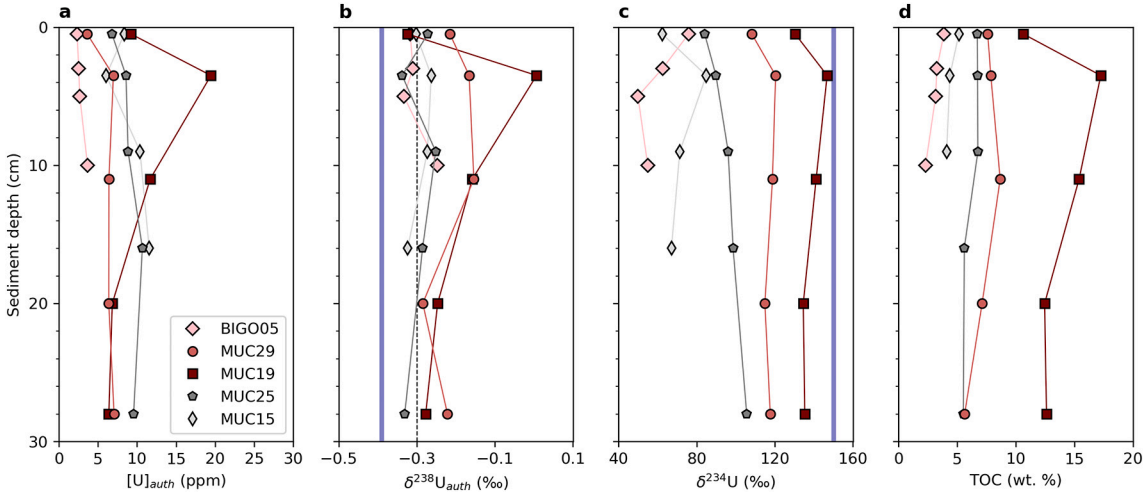

Fig. 2. Depth profiles. Depth profiles of the Peruvian margin, illustrating a) sedimentary authigenic U concentrations (U_{auth}), b) $\delta^{238}U_{auth}$ values, c) $\delta^{234}U$ values of bulk sediments and d) TOC (TOC data from Scholz et al. (2011)). The blue bars indicate seawater $\delta^{238}U$ (−0.39‰) or $\delta^{234}U$ values (147‰), the black dashed line the average detrital $\delta^{238}U$ value (−0.3‰; Andersen et al., 2014).

Table 2
Uranium isotope and concentration data of bulk sediment samples.

Station	Sediment depth	$\delta^{238}U_{bulk}$	2SD	$\delta^{234}U_{bulk}$	2SD	n	TOC	Al	U	U/Al	U_{auth}	f_{det}	$\delta^{238}U_{auth}$	$\Delta^{238}U$	U_{PNU}[a]
	(cm)	(‰)		(‰)			(wt %)	(ppm)	(ppm)	(ppm / ppm) * 10^3	(ppm)		(‰)	(‰)	(%)
BIGO05	0.5	−0.31	0.07	76	3	1	3.9	52,145	3.28	0.063	2.34	0.29	−0.32	0.07	28
	3	−0.31	0.07	62	1	2	3.3	64,289	3.69	0.057	2.53	0.31	−0.31	0.08	22
	5	−0.32	0.04	50	4	4	3.2	70,421	3.94	0.056	2.67	0.32	−0.33	0.06	20
	10	−0.26	0.12	55	3	6	2.3	69,837	4.92	0.070	3.66	0.26	−0.25	0.14	11
MUC29	0.5	−0.23	0.07	108	3	1	7.6	45,598	4.44	0.097	3.62	0.18	−0.22	0.17	36
	3.5	−0.18	0.07	120	3	1	7.9	50,872	7.89	0.155	6.97	0.12	−0.17	0.22	19
	11	−0.17	0.08	119	4	2	8.7	47,757	7.26	0.152	6.40	0.12	−0.15	0.24	23
	20	−0.29	0.08	115	0	2	7.1	50,481	7.29	0.144	6.38	0.12	−0.28	0.11	19
	28	−0.23	0.02	118	2	2	5.6	50,041	7.96	0.159	7.06	0.11	−0.22	0.17	14
MUC19	0.5	−0.32	0.07	130	1	2	10.7	32,627	9.82	0.301	9.23	0.06	−0.32	0.07	20
	3.5	0.00	0.01	147	2	4	17.3	21,498	19.84	0.923	19.5	0.02	0.01	0.40	15
	11	−0.16	0.03	141	3	4	15.4	17,855	12.00	0.672	11.7	0.03	−0.16	0.23	22
	20	−0.25	0.03	135	3	4	12.5	22,682	7.24	0.319	6.83	0.06	−0.25	0.14	31
	28	−0.28	0.06	135	1	4	12.6	21,434	6.77	0.316	6.39	0.06	−0.28	0.11	34
MUC41	surface	−0.52	0.03	−57	7	4			30.28					−0.13	
	surface	−0.47	0.06	−21	1	4			73.83					−0.08	
	surface	−0.80	0.12	42	1	4			6.80					−0.41	
MUC25	0.5	−0.27	0.09	84	3	4	6.7	36,375	7.44	0.205	6.79	0.09	−0.27	0.12	17
	3.5	−0.33	0.10	90	3	5	6.7	39,599	9.29	0.235	8.58	0.08	−0.34	0.05	13
	9	−0.25	0.04	96	1	3	6.8	37,367	9.53	0.255	8.86	0.07	−0.25	0.14	13
	16	−0.29	0.04	99	3	5	5.6	45,324	11.49	0.254	10.68	0.07	−0.29	0.10	9
	28	−0.33	0.08	106	1	4	5.5	45,412	10.38	0.228	9.56	0.08	−0.33	0.06	10
MUC15	0.5	−0.30	0.09	62	1	3	5.2	41,407	9.11	0.220	8.36	0.08	−0.30	0.09	10
	3.5	−0.27	0.06	85	4	4	4.4	39,503	6.76	0.171	6.05	0.11	−0.26	0.13	12
	9	−0.27	0.02	71	1	4	4.1	41,971	11.14	0.265	10.38	0.07	−0.27	0.12	7
	16	−0.32	0.02	67	3	3	N/A	38,214	12.24	0.320	11.55	0.06	−0.32		

[a] U_{PNU} is calculated based on the data from Holmden et al. (2015), using a U_{PNU}/TOC ratio of 0.17 ppm/wt%.

concentrations increasing with sediment depth, except for MUC19, where U_{auth} peaks at 3.5 cm sediment depth (Fig. 2a). This peak co-occurs with high TOC (data from Scholz et al., 2011; Fig. 2d) and likely indicates a peak in export production, leading to high TOC and U_{auth} (Salvatteci et al., 2014). However, this co-variation of TOC and U_{auth} could also be an indirect relationship since TOC drives microbial metabolism and thus, U reduction (Klinkhammer and Palmer, 1991; Morford et al., 2009). The relationship of this U_{auth} peak with organic matter is further supported by the good correlation between U_{auth} and TOC for the persistently anoxic station (R^2 = 0.70; Fig. 4a). This observation indicates that besides diffusive U input, a proportion of U can reach the sediment as particulate input in association with organic matter. Indeed, particulate U input, specifically as PNU, has been proposed as a source of authigenic U (e.g. Zheng et al., 2002a; Zheng et al., 2002b; Scholz et al., 2011).

Uranium isotope compositions in sediments are typically interpreted to reflect the redox state of bottom water (e.g. Andersen et al., 2014a). In agreement with this interpretation, the $\delta^{238}U_{auth}$ values of our sediment samples deposited under oxic conditions are typically isotopically lighter (−0.34 to −0.25‰; Fig. 2b, Table 2) compared with samples deposited in anoxic, non-sulfidic bottom waters (−0.33 to 0.01‰). Below the OMZ (sites MUC25 and MUC15), under oxic conditions in the bottom water, the average $\delta^{238}U_{auth}$ value is closer to seawater (average $\Delta^{238}U_{auth\text{-}seawater}$ = 0.10 ± 0.07‰, n = 8) compared with samples deposited under anoxic, non-sulfidic conditions with $\Delta^{238}U_{auth\text{-}seawater}$ values of 0.07‰ to 0.40‰ (BIGO05, MUC29, MUC19). We note that sediments deposited under anoxic, non-euxinic conditions such as the ones investigated here show a higher degree of effective isotope fractionation from seawater compared to oxic sediments. This observation confirms the modelled isotope offset of less than 0.6‰ under anoxic, non-sulfidic conditions (Andersen et al., 2014a). Compared to sulfidic sediments from euxinic basins, our data from an anoxic, non-euxinic setting show a lower degree of effective isotope fractionation. For example, in the euxinic Black Sea, the $\Delta^{238}U_{auth\text{-}seawater}$ is 0.63‰ (Rolison et al., 2017). However, we recognise the differences between the Peruvian margin and the Black Sea which may limit the comparability. Still, this observation is also in agreement with Cole et al. (2020) who showed a lower degree of isotope fractionation during U removal to ferruginous sediments compared to sediments in euxinic settings.

Not all sediment samples from the Peruvian margin exposed to anoxic bottom water show increased $\delta^{238}U$ values compared with samples deposited under oxic conditions. The samples from the anoxic shelf (BIGO05 at 85 m water depth and MUC29 at 145 m; $\delta^{238}U_{auth}$ values between −0.33‰ and − 0.15‰) are similar to samples deposited under oxic conditions. These two cores likely experience elevated bottom water oxygen conditions when the oxycline is deepened due to coastal trapped waves (Gutiérrez et al., 2008). We hypothesise that these occasional redox changes and low rates of U reduction and fractionation during oxic periods keep $\delta^{238}U_{auth}$ values low, masking the generally anoxic conditions. Similarly, large variations in U isotope compositions were observed in sediments in the Baltic Sea and the Black Sea, where redox states were subject to recent changes, e.g. due to flushing events (Andersen et al., 2014a; Noordmann et al., 2015).

In a previous study of core top sediment samples from the Peruvian margin, Cole et al. (2020) observed overlapping $\delta^{238}U$ values for sediments deposited under oxic or anoxic ferruginous conditions. Their observation is in agreement with some of our surface samples which show that oxic and anoxic sediments can have overlapping $\delta^{238}U$ values in the absence of bottom water H_2S. At the anoxic sites, however, we observe increases in U_{auth} concentrations and $\delta^{238}U$ values with depth, suggesting that the continued uptake of U during early diagenesis acts to modify the U isotope compositions in response to sedimentary redox conditions before they become part of the sediment paleo-record.

Especially under persistently anoxic conditions, we observe higher $\delta^{238}U_{auth}$ values in the upper 10 cm of the sediment compared with sediments deposited under oxic conditions. The increase in $\delta^{238}U$ values with depth can be caused by the high rate of seawater-derived U reduction favouring isotopically heavy U, leading to an enrichment of isotopically heavy U and thus high $\delta^{238}U_{auth}$ values in the sediment (Weyer et al., 2008; Andersen et al., 2014a). However, we provide

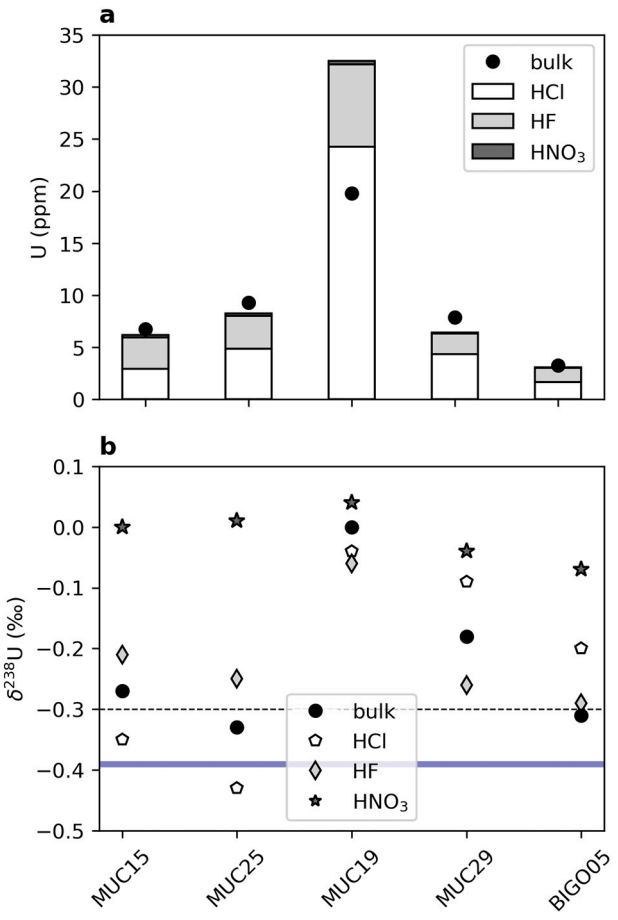

Fig. 3. Sequential extraction. Plot a) shows U concentrations, where vertical bars depict cumulative U concentrations in each sequentially extracted sediment fraction for one sediment sample (0.5 or 3.5 cm sediment depth) from each of our site on the Peruvian margin. The circles indicate the U concentration measured in bulk samples. The U concentration of the HNO_3-leachable fraction in BIGO05 is lower than the thickness of the lines of the bar. Plot b) shows U isotope compositions of sequential extractions for the same samples. The blue horizontal bar indicates the global seawater $\delta^{238}U$ value, the black dashed line the average detrital $\delta^{238}U$ value.

additional data (TOC, sequential extraction) that support a second mechanism of (isotopically heavy) U delivery to the sediment which is discussed below.

4.2. Diffusive and particulate input

The reduction of U in the surface sediment under anoxic conditions is generally accepted as the main mechanism driving U accumulation in sediments (e.g. Klinkhammer and Palmer, 1991). However, U can also be transported to the sediment by particles (e.g. Anderson et al., 1989b; Zheng et al., 2002a). Across the Peruvian margin, diffusion of U into the sediment alone cannot explain the U accumulation (Scholz et al., 2011). Indeed, authigenic U mass accumulation rates (MAR) and benthic fluxes suggest that diffusion of U is typically not sufficient to supply authigenic U in our sediments (Scholz et al., 2011).

In the sediment samples in the persistently anoxic core (MUC19) with the highest TOC content (up to 17.3 wt%; Scholz et al., 2011), we observe a good correlation between U_{auth} concentrations and TOC ($R^2 = 0.70$; Fig. 4a). Two possible pathways can explain this positive correlation. 1) Efficient U reduction mediated by microorganisms directly below the sediment-water interface of organic-rich sediments, and 2) shuttling of U to the sediment with sinking organic matter, e.g. PNU. A positive correlation between TOC and $\delta^{238}U_{auth}$ values as in the MUC19 core ($R^2 = 0.94$; Fig. 4b) was previously observed under anoxic conditions on the Namibian continental margin (Abshire et al., 2020). This correlation suggests that microbially reduced U is fractionated towards heavier isotope compositions. However, we cannot exclude particulate U input in the MUC19 core based on our data set.

Table 3
Sequential extraction data for one surface sediment sample (0.5 or 3.5 cm sediment depth) from each site.

Fraction	Sediment depth	U	$\delta^{238}U$	2SD	$\delta^{234}U$	2SD	n
	(cm)	(ppm)	(‰)		(‰)		
reactive	0.5	1.65	−0.20	0.12	147	9	3
silicate		1.37	−0.29	0.11	104	4	2
HNO_3-soluble		0.06					
calculated total		3.07					
measured bulk		3.28	−0.31				
reactive	3.5	4.35	−0.09	0.02	147	11	4
silicate		1.99	−0.26	0.20	107	1	2
HNO_3-soluble		0.06					
calculated total		6.40					
measured bulk		7.89	−0.18				
reactive	3.5	24.3	−0.04	0.04	147	9	4
silicate		7.91	−0.06	0.07	135	2	3
HNO_3-soluble		0.32					
calculated total		32.5					
measured bulk		19.8	0.00				
reactive	3.5	4.84	−0.43	0.02	134	1	3
silicate		3.18	−0.25	0.12	49	3	4
HNO_3-soluble		0.23					
calculated total		8.24					
measured bulk		9.29	−0.33				
reactive	3.5	2.94	−0.35	0.06	132	1	3
silicate		3.03	−0.21	0.04	63	6	4
HNO_3-soluble		0.19					
calculated total		6.16					
measured bulk		6.76	−0.27				

In most of our stations, the benthic diffusive fluxes of U cannot account for the corresponding MAR of U, indicating that diffusive U accumulation is not the only pathway of U delivery to the sediment (Scholz et al., 2011). Organic matter such as plankton has very low U concentrations, indicating that only a small proportion of U is incorporated into the organisms (Holmden et al., 2015). Instead, these authors suggest that the U in/on particulate matter in the water column is added while particles are settling (i.e. scavenged) as live plankton contributes very little to the U in sediment traps (2%). Uranium associated with organic matter or inorganic particles settling through the water column is fractionated by a two-step mechanism (Holmden et al., 2015; Basu et al., 2020). This mechanism includes 1) sorption of U onto settling organic particles and 2) reduction of U(VI) to U(IV) inducing a positive fractionation.

To investigate whether delivery of U through organic particles can contribute U with elevated isotope composition (relative to seawater), we turn to the data of Holmden et al. (2015) from the oxygen-deficient Saanich Inlet. Their sediment trap data reveal that U is incorporated into settling particles, likely through sorption. We calculate a U_{PNU}/TOC ratio of 0.17 ppm/wt% based on their data, using their sediment trap U concentrations and seawater U fractions ($f_{seawater}$) to calculate U_{PNU} (Tables 2 and 4). Applying this ratio to our sediment U and TOC data, we estimate that up to 36% of U at our anoxic sites (BIGO09, MUC19 and

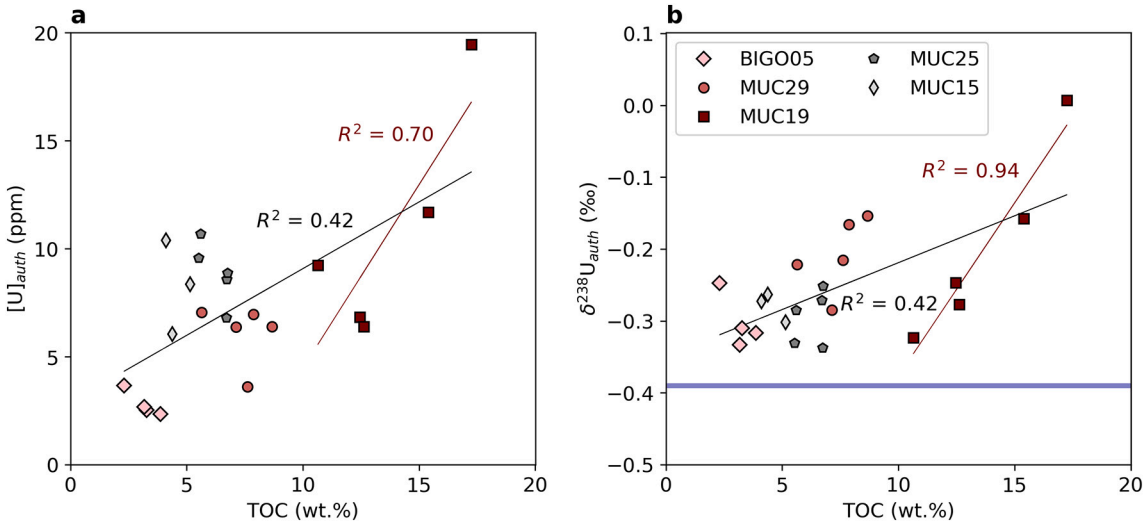

Fig. 4. Correlation of U with TOC. Cross-plots of a) U_{auth} concentrations and b) $\delta^{238}U_{auth}$ values with TOC. The red correlation lines and R^2 refer to the permanently anoxic core (MUC19), the black correlation lines and R^2 include all samples. The blue bar indicates the global seawater $\delta^{238}U$ value.

Table 4
Isotope mass balance using data from Holmden et al. (2015) to calculate the U isotope composition of PNU in Saanich Inlet samples.

Sample	Depth		TOC	U	$\delta^{238}U$	2SE	f_{SW}	1 - f_{SW}	U_{PNU}	U_{PNU}/TOC	$\delta^{238}U_{PNU}$	$\Delta^{238}U_{PNU\text{-}SW}$
	(m)		(wt%)	(ppm)	(‰)	(‰)			(ppm)	(ppm/wt%)	(‰)	(‰)
January/February												
	Shallow	50	7.10	2.04	−0.52		0.21	0.79	0.43	0.06	0.65	1.10
	Mid	115	4.90	1.67	−0.66	0.01	0.19	0.81	0.32	0.06	0.06	0.51
	Deep	180	4.70	1.96	−0.58	0.10	0.27	0.73	0.53	0.11	0.10	0.55
March												
	Deep	180	3.60	2.10	−0.29		0.42	0.58	0.88	0.25	0.46	0.91
April												
	Mid	115	3.80	1.98	−0.51	0.16	0.41	0.59	0.81	0.21	−0.05	0.40
	Deep	180	4.10	2.90	−0.56	0.23	0.42	0.58	1.22	0.30	−0.19	0.26
Average ± 2SD										0.17 ± 0.20	0.17 ± 0.63	0.62 ± 0.63

SW = seawater; f_{SW} represents the seawater-derived U fraction, $\delta^{238}U_{PNU}$ is calculated using 1 − f_{SW} and $\delta^{238}U_{detrital}$ value of −0.83 ± 0.12 (2σ) ‰, $\delta^{238}U$ value of seawater endmember: −0.45 ± 0.06 (2σ) ‰.

MUC29), and 7 to 17% at the oxic sites (MUC25 and MUC15) may be derived from PNU (Table 2). These estimates confirm that U delivered through PNU may constitute a sizable proportion of authigenic U, especially for anoxic sediments.

Next, we use an isotope mass balance to calculate the U isotope composition of PNU in the Saanich Inlet samples (Eq. 4). Based on the local detrital $\delta^{238}U$ value and measured bulk U isotope composition of sediment trap samples, we calculate an average $\delta^{238}U$ value for PNU ($\delta^{238}U_{PNU}$) of 0.17 ± 0.63‰ (2SD; Table 4). Note that the isotope composition of the detrital component in the Saanich Inlet sediments is unusual light (−0.83‰), which the authors attribute to fractionation of U during soil processes and weathering, where altered minerals preferentially retain the lighter U isotopes (Holmden et al., 2015). Compared to the U isotope composition of −0.45‰ for Saanich Inlet seawater, our calculations suggest that U incorporation into settling particles can deliver PNU that is similar to or heavier than the seawater source. The average isotope offset between PNU and seawater ($\Delta^{238}U_{PNU\text{-}seawater}$) is 0.62 ± 0.63‰ (2SD), which is similar to the isotope effect determined for the Black Sea water column based on dissolved U isotope compositions (Romaniello, 2012). Further, the isotope offset is in the range of experimentally determined isotope fractionation effects of microbial U (VI) reduction (Basu et al., 2014; Stirling et al., 2015). It has been speculated that U reduction occurs in settling particles within the water column (e.g. Anderson et al., 1989a; Rolison et al., 2017). In support, under reducing lacustrine conditions, progressive accumulation of isotopically heavy U in sinking particles with water depth was recently described (Chen et al., 2021). These authors attribute this trend to U(VI) reduction. We note, however, that direct measurements of U redox speciation in the Black Sea water column did not provide any evidence for U(VI) reduction, despite the presence of free H_2S (Anderson et al., 1989a). Also, the highest $\Delta^{238}U_{PNU\text{-}seawater}$ for the Saanich Inlet (1.10‰) was calculated for the surface sediment trap (Table 4), well above the redoxcline (Holmden et al., 2015), thus making a reductive pathway for U uptake unlikely in this sample.

Alternatively, isotope fractionation may occur during sorption onto phytoplankton. However, studies of marine and freshwater phytoplankton suggest that U(VI) sorbed onto living surface plankton fractionates in the opposite direction ($\Delta^{238}U_{plankton\text{-}seawater}$ = −0.79‰ for marine and − 0.23‰ for freshwater plankton; Holmden et al., 2015; Chen et al., 2020) than is implied by the deeper sediment trap PNU in the Saanich Inlet. The mechanism for the uptake and elevated U isotope composition in sinking particles on the Peruvian margin, therefore, remains speculative and warrants further investigation that must include direct determination of U redox speciation in dissolved and particulate U phases.

Uranium that settles to the sediment with organic particles is redistributed during early diagenesis under oxic conditions (Zheng et al., 2002a). Within anoxic sediment, early diagenesis leads to degradation of organic matter, releasing both surface-bound and incorporated U into the porewater (Scholz et al., 2011). With the subsequent microbial reduction and precipitation of U_{auth}, U initially associated with organic matter is diagenetically redistributed into an authigenic host fraction.

The reduction of U induces a fractionation of U, leading to preferential enrichment of isotopically heavy U in the authigenic phase. Our data support the hypothesis that input of PNU with sinking organic matter plays an important role in the delivery of U to the sediments (Scholz et al., 2011). Further, we hypothesise that U reduction during early diagenetic redistribution into permanent mineral phases such as uraninite ultimately determines the isotope composition of buried U_{auth}. This reduction process is more important in organic-rich compared to organic-poor sediments.

While our dataset supports the idea that both diffusive and particulate U input affect the sediment U isotope mass budget, we cannot separate the U isotope fractionation effects of diffusive and particulate U input. Our data suggest that both of these processes seem to favour the incorporation of isotopically heavy U into the sediment. However, diffusive vs. particulate U input may lead to differences in the U isotope composition of the sediment, as previously suggested for the Mo isotope system (Eroglu et al., 2020). Although Andersen et al. (2017) suggested that U reduction can take place above the sediment-water interface, this process is poorly constrained in natural environments. Using a transport model, Lau et al. (2020) linked $\delta^{238}U$ values in sediments with productivity and, thus, C_{org} burial rates. Changes in diffusive vs. particulate U input, e.g. linked to changes in sedimentation and C_{org} rain and burial rates, in the geological past can affect the global U isotope mass budget.

4.3. Uranium-hosting sediment fractions

4.3.1. Reactive fraction

Authigenic U may best be represented by the reactive fraction (0.5 M HCl), which includes mineral phases that precipitated directly from the water column or porewater (e.g. Fe- and Mn-oxyhydroxides, carbonates, hydrous aluminosilicates, and Fe monosulfides; Huerta-Diaz and Morse, 1990). Additionally, this fraction may also include U leached from particle surfaces, including PNU and U sorbed onto organic matter. An authigenic origin of the reactive fraction in our sequential extracts is supported by the high $\delta^{234}U_{reactive}$ values of all five surface samples (142 ± 16 (2SD) ‰) that are very close to the seawater $\delta^{234}U$ value (147‰). The $\delta^{234}U_{reactive}$ values of the two sediment cores deposited under oxygenated bottom water (MUC25 and MUC15) have slightly lower $\delta^{234}U_{reactive}$ values compared to anoxic cores (e.g. MUC19), possibly due to dissolution of CFA during the HCl leach. Low $\delta^{234}U$ values in phosphorite nodules −57 ± 7‰ to 42 ± 1‰ at oxic station MUC41 suggest that CFA $\delta^{234}U$ isotope compositions deviate significantly from seawater values, despite being an authigenic mineral phase.

Our $\delta^{238}U$ isotope analyses show a clear distinction between $\delta^{238}U_{reactive}$ values in sediments deposited under oxic (average − 0.39 ± 0.06 (2SD) ‰, $n = 2$) versus under anoxic conditions (average − 0.07 ± 0.04 (2SD) ‰, n = 2). The two sediment cores deposited under the highest bottom water oxygen concentrations at our sites (MUC25; 12 μm and MUC15: 40 μM; Table 1) show $\delta^{238}U_{reactive}$ values (−0.43 ± 0.02‰ and − 0.35 ± 0.06‰, respectively) close to the seawater $\delta^{238}U$ value (−0.39 ± 0.01‰; Andersen et al., 2014a, Tissot and Dauphas, 2015). Under anoxic bottom water conditions (excluding BIGO05), the reactive fraction is clearly fractionated towards higher $\delta^{238}U$ values (−0.20‰ or higher) compared with oxic conditions. This distinct difference between oxic and anoxic sites is in agreement with the proposed model that under oxic bottom water conditions, U reduction occurs deeper in the sediment, where the resulting diffusive U flux from bottom water to sediment leads to a small to no isotope offset (Andersen et al., 2014a). Bioturbation at the oxic sites would also contribute to maintaining the supply of U with low isotope composition to several cm depth. The isotope compositions of sediments deposited under anoxic vs. oxic conditions show more pronounced differences in the reactive fraction ($\delta^{238}U_{reactive}$) of the sediment compared with calculations of authigenic U ($\delta^{238}U_{auth}$), suggesting that the reactive fraction is more accurate in recording the long-term redox conditions of the bottom water than $\delta^{238}U_{auth}$ values.

4.3.2. Silicate fraction

The silicate fraction has in $\delta^{238}U$ values (~ −0.25‰) similar to the continental crust (−0.3‰; Weyer et al., 2008), except for the sample from the persistent OMZ (MUC19) which has a value of −0.06‰. The silicate fraction from this core deviates from the other locations in both $\delta^{238}U$ and $\delta^{234}U$ values. The $\delta^{234}U$ values of the silicate fractions for anoxic site MUC19 display values close to seawater (135 ± 2‰), suggesting that this fraction includes an authigenic mineral phase that was insufficiently removed during the leaching step with 0.5 M HCl. This non-silicate phase may include crystalline Fe-oxide minerals (e.g. goethite and lepidocrocite), which was not dissolved by the relatively mild HCl leach. Previous leaching experiments (Severmann, unpublished data) suggest that HF is an effective solvent for crystalline Fe-oxides, which may have formed from amorphous Fe-oxide precursors. Alternatively, sediments at this site may include a higher proportion of biogenic silica.

4.3.3. HNO_3-soluble fraction

The HNO_3-soluble fraction supposedly contains U associated with organic matter and pyrite. However, U contained in the HNO_3-soluble fraction does not seem to play a major role in the U budget on the Peruvian margin. This can be concluded from several observations. First, the U contained in the HNO_3-soluble fraction contributes ≤3.2% of the U_{auth}. Second, overall U_{auth} concentrations and TOC do not show a strong correlation ($R^2 = 0.42$), except for a positive correlation for the samples from persistently anoxic conditions (MUC19; $R^2 = 0.70$). This correlation for MUC19 is even more prominent when comparing $\delta^{238}U_{auth}$ values and TOC ($R^2 = 0.94$). This trend indicates that, despite the low U content of the HNO_3-soluble fraction, U isotope compositions under persistently anoxic conditions on the Peruvian margin are strongly influenced by organic matter.

Redistribution of U during early diagenesis, as well as imperfect separation of U during successive leaching steps, can explain the low U concentrations in the HNO_3-soluble fraction. Uranium associated with organic matter through surface sorption or incorporation during particle settling (e.g. Holmden et al., 2015) may be incorporated into the authigenic (HCl-leachable) fraction during early diagenetic redistribution. Additionally, during sequential extraction, weak HCl may leach U from organic matter. Hence, it is possible that a proportion of U associated with organic matter is actually comprised in the reactive fraction rather than in the HNO_3-soluble fraction. In the absence of further testing, we are unable to distinguish between the two options. Given the known role of microbial reduction in fixing authigenic U in anoxic sediments (e.g. Klinkhammer and Palmer, 1991) we prefer the former explanation.

4.3.4. Phosphorites

The isotope composition of U in phosphorites indicates that U in this authigenic mineral phase underwent significant changes during its pathway from seawater to phosphorite, leading to pronounced isotope offsets between seawater and phosphorites ($\Delta^{238}U_{phosphorite\text{-}seawater}$ values of between −0.41 and − 0.08‰; Table 2). The U isotope offsets between seawater and phosphorites can be explained by the formation history of phosphorite nodules during early diagenesis. While U can reach the sediment with sinking organic matter such as PNU, it is unlikely that PNU is buried without further alteration in the sediment. Instead, U is redistributed during early diagenesis and accumulates in phosphorite crusts downslope (e.g. Scholz et al., 2011; Böning et al., 2004).

In upwelling zones, where the conditions in the surface sediments are suboxic, P can be released to the dissolved phase at the sediment-water interface (e.g. from organic matter or Fe oxides). Consequently, porewater can be supersaturated in CFA, leading to precipitation of CFA (e.g. Froelich et al., 1988). On the Peruvian margin, CFA can precipitate on the shelf, e.g. in BIGO05 or MUC29. Due to the low $\delta^{238}U$ values of the phosphorites (−0.80‰ to −0.47‰), we propose that precipitation of

CFA during early diagenesis favours the lighter U isotopes (^{235}U over ^{238}U). Due to (episodically) high-energy conditions, CFA coated grains are eroded and transported downslope, where they are re-deposited (Reimers and Suess, 1983; Glenn and Arthur, 1988; Arning et al., 2009). Under oxic conditions (MUC15 and MUC25), the growth of new CFA layers can continue, leading to the formation of phosphorite crusts (Arning et al., 2009).

The $\delta^{234}U$ values of phosphorites (-57 ± 7‰ to 42 ± 1‰) are clearly offset from the seawater $\delta^{234}U$ value. Since CFA coated grains formed upslope and were later transported downslope, we assume that the source of U in the phosphorites is older compared with other sediment fractions in the same core and sediment depth. In addition, the negative $\delta^{234}U$ values suggest that ^{234}U has been preferentially lost from this mineral phase, likely due to diagenetic overprinting. Post-depositional remobilisation of ^{234}U suggests that the $\delta^{234}U$ was also affected by diagenetic overprinting, i.e. that these phases do not represent seawater isotope composition. A significantly older age can explain $\delta^{234}U$ values close to zero assuming closed system radiogenic ingrowth (Henderson, 2002). Alternatively, ^{234}U is gradually lost from phosphorites during diagenesis by alpha recoil during their life span, which can cause their low $\delta^{234}U$ values (Henderson, 2002). The $\delta^{234}U$ data of sediments other than phosphorites further support redistribution of U. High $\delta^{234}U$ values similar to seawater in the most anoxic core (MUC19) suggest that U in these samples did not undergo substantial loss of ^{234}U due to alpha recoil and diagenetic overprinting. This observation indicates that U in this core was less affected by remobilisation (e.g. during the redistribution of U during phosphorite formation) compared with the two other anoxic cores (MUC29 and BIGO05). Alternatively, other processes, e.g. particulate U input under persistently anoxic conditions, may have had a stronger impact on U in this sediment core. The $\delta^{234}U$ values of BIGO05 indicate extensive loss of ^{234}U, possibly due to high rates of U remobilisation under episodically oxic conditions (Severmann and Thomson, 1998). Moreover, $\delta^{234}U$ values of bulk sediments deposited under oxic conditions (MUC15 and MUC25) are substantially lower than in the anoxic cores (MUC19 and MUC29), supporting that further upslope, U (preferentially ^{234}U) is remobilised from the sediment and accumulates downslope.

5. Implications for paleo-reconstructions

Cycling of U on the Peruvian margin is schematically illustrated in Fig. 5, providing a model of U cycling in a modern open marine environment. Under reducing conditions in the OMZ, sedimentary $\delta^{238}U$ values are higher compared to seawater, with the highest values found under persistently anoxic conditions. Across the Peruvian margin, U accumulates in the sediment both via diffusive and particulate input. The correlation between TOC and $\delta^{238}U$ values in the permanent OMZ (MUC19) indicates that organic-rich sediments preferentially accumulate isotopically heavy U, through the delivery of organic particles with elevated $\delta^{238}U$ values combined with U reduction within the sediment mediated by microorganisms. With the degradation of organic matter and regeneration of PNU under oxic conditions, associated (isotopically heavy) U can be released into the porewater, from where it precipitates (upon reduction) and accumulates as authigenic U (Scholz et al., 2011). This reworking mechanism can be observed in our isotope analyses, where heavy U isotopes remain in the reactive fraction of the sediment. Light U isotopes are preferentially incorporated into precipitating CFA grains, which are transported downslope and eventually form phosphorite crusts. In sediments deposited under oxic conditions, the $\delta^{238}U_{auth}$ values are similar to typical seawater values, and lower compared with sediments deposited under anoxic, non-euxinic conditions.

Our dataset, investigating the U isotope compositions in modern anoxic and typically non-sulfidic sediments, helps to better constrain the interpretations of U isotope data from the geological record. Reconstructions of the extent of anoxic seafloor typically work with the assumption that the largest effective U isotope fractionations are associated with anoxic sediments (e.g. Zhang et al., 2018). The data from the Peruvian margin show that anoxic sediments do not necessarily record a large offset from seawater. Instead, the offset between sediments and the overlying water column in an anoxic, non-euxinic setting ($\Delta^{238}U_{authigenic\text{-}seawater}$ between 0.07 and 0.40‰) is smaller than under euxinic conditions (>0.6‰; Basu et al., 2014; Rolison et al., 2017), but larger than under oxic conditions (e.g. Basu et al., 2014). Furthermore, our data indicate that TOC and thus, C_{org} rain and burial rates, also influence the U isotope composition of the sediments. Consequently, large effective U isotope fractionations are not necessarily associated with anoxic conditions in general, but instead, fractionation depends on other factors such as the presence or absence of H_2S in and above porewaters, and C_{org} rain and burial rates. Nevertheless, euxinic sediments seem to induce the largest degree of U isotope fractionation of all known U sinks, including anoxic, non-sulfidic sediments. Thus, large U isotope fractionation factors in ancient sedimentary rocks are likely recording the extent of euxinia, rather than anoxia in general.

6. Conclusions

We investigated U biogeochemical cycling under a range of redox

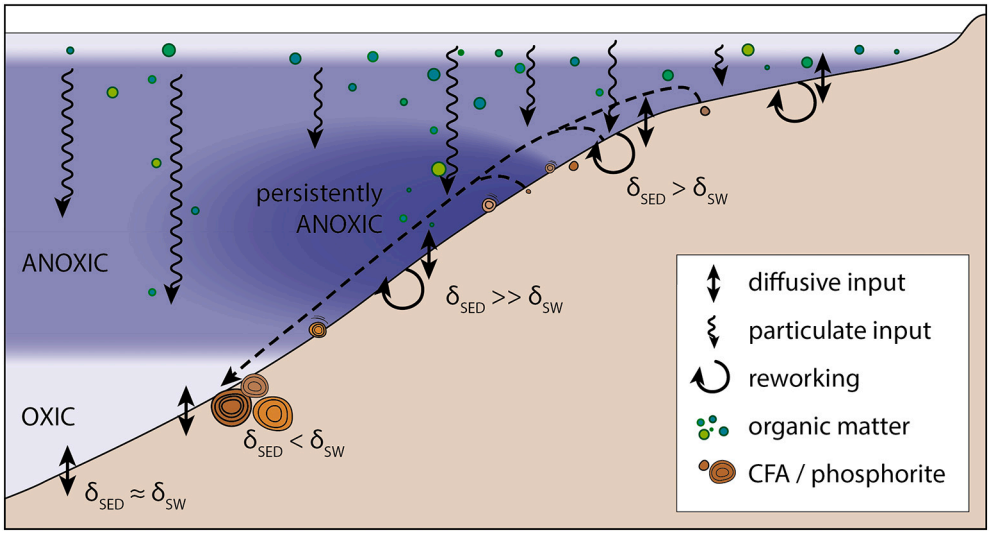

Fig. 5. Schematic overview. Schematic of U cycling on the Peruvian margin. The OMZ is indicated in blue, with a darker shade for the permanently anoxic core. Uranium input into sediment can take place via a diffusive (double-headed arrow) or particulate pathway (zigzag arrow). Both of these processes are thought to preferentially deliver heavy U isotopes. During early diagenesis, organic matter is decomposed and associated U is likely redistributed. Heavier isotopes are thought to remain in an authigenic phase of the sediment where U(VI) reduction occurs ($\delta_{SED} > \delta_{SW}$). Lighter U isotopes are preferentially incorporated into CFA grains, which may be transported downslope (dashed arrow), re-depositing as phosphorite crusts below the OMZ ($\delta_{SED} < \delta_{SW}$). The sediment deposited under oxic conditions below OMZ has U isotope compositions similar to seawater ($\delta \approx \delta_{SW}$).

conditions in a non-euxinic open ocean environment with high productivity. The $\delta^{238}U_{auth}$ values in sediments record mixed signals with contributions from organic matter rain from the water column and redox-related processes in the sediments. Particulate and diffusive input of U, both tightly linked to organic matter, can affect U concentrations and their isotope compositions. Our data show that bottom water redox state impacts $\delta^{238}U_{auth}$ values, although differences between $\delta^{238}U_{auth}$ values deposited under anoxic and oxic conditions can be small. The results of our sequential extractions show that the reactive sediment fraction is more sensitive to reliably record the redox state of ambient seawater than $\delta^{238}U_{auth}$ values calculated from major ion chemistry. The applicability of our method to extract the reactive fraction (weak HCl leach) on shales remains to be investigated.

The U isotope offset between anoxic, non-sulfidic sediments and seawater constrained here (<0.40‰) is smaller compared with the offset observed in euxinic environments, but can be larger than the offset in oxic environments depending on the organic content of the anoxic, non-sulfidic sediments. Thus, large U isotope fractionation factors inferred for anoxic sediments, which inform estimates of ancient ocean anoxia from the sedimentary rock record, cannot universally be applied for all anoxic environments. Instead, the presence or absence of H_2S in and above porewaters, as well as C_{org} rain and burial rates, driving the TOC content of the sediment, also affect U isotope fractionation. These findings allow us to better constrain ancient ocean conditions from the sedimentary U isotope record, further defining the abundance of anoxic ocean conditions in Earth history.

Declaration of Competing Interest

The authors declare that they have no known competing financial interests or personal relationships that could have appeared to influence the work reported in this paper.

Acknowledgement

This work was supported by the German Research Foundation (Sonderforschungsbereich 754, "Climate-Biogeochemistry Interactions in the Tropical Ocean" and Emmy Noether Nachwuchsforschergruppe ICONOX, "Iron cycling in continental margin sediments and the nutrient and oxygen balance of the ocean"); the European Union's Horizon 2020 research and innovation programme (grant agreement No 643084); the NASA Postdoctoral Program; the NSF (grant OC-1657690); and the Villum Foundation (grant number 16518).

References

Abshire, M.L., Romaniello, S.J., Kuzminov, A.M., Cofrancesco, J., Severmann, S., Riedinger, N., 2020. Uranium isotopes as a proxy for primary depositional redox conditions in organic-rich marine systems. Earth Planet. Sci. Lett. 529, 115878.
Algeo, T.J., Tribovillard, N., 2009. Environmental analysis of paleoceanographic systems based on molybdenum – uranium covariation. Chem. Geol. 268, 211–225.
Andersen, M.B., Stirling, C.H., Zimmermann, B., Halliday, A.N., 2010. Precise determination of the open ocean 234U/238U composition. Geochem. Geophys. Geosyst. 11, 1–8.
Andersen, M.B., Romaniello, S., Vance, D., Little, S.H., Herdman, R., Lyons, T.W., 2014. A modern framework for the interpretation of 238U/235U in studies of ancient ocean redox. Earth Planet. Sci. Lett. 400, 184–194.
Andersen, M.B., Stirling, C.H., Potter, E.K., Halliday., A.N., 2004. Toward epsilon levels of measurement precision on 234U/ 238U by using MC-ICPMS. Int. J. Mass Spectrom. 237, 107–118.
Andersen, M.B., Stirling, C.H., Weyer, S., 2017. Uranium isotope fractionation. Rev. Mineral. Geochem. 82, 799–850.
Anderson, R.F., Fleisher, M.Q., Lehuray, A.P., Doherty, L., Observatory, G., Ny, U.S.A., 1989a. Concentration, oxidation state, and particulate flux of uranium in the Black Sea. Geochim. Cosmochim. Acta 53.
Anderson, R.F., LeHuray, A.P., Fleisher, M.Q., Murray, J.W., 1989b. Uranium deposition in Saanich Inlet sediments, Vancouver Island. Geochim. Cosmochim. Acta 53, 2205–2213.
Arning, E.T., Lückge, A., Breuer, C., Gussone, N., Birgel, D., Peckmann, J., 2009. Genesis of phosphorite crusts off Peru. Mar. Geol. 262, 68–81.
Barnes, C.E., Cochran, J.K., 1990. Uranium removal in oceanic sediments and the oceanic U balance. Earth Planet. Sci. Lett. 97, 94–101.
Basu, A., Sanford, R.A., Johnson, T.M., Lundstrom, C.C., Lo, F.E., 2014. Uranium isotopic fractionation factors during U (VI) reduction by bacterial isolates. Geochim. Cosmochim. Acta 136, 100–113.
Basu, A., Wanner, C., Johnson, T.M., Lundstrom, C.C., Sanford, R.A., Sonnenthal, E.L., Boyanov, M.I., Kemner, K.M., 2020. Microbial U Isotope Fractionation Depends on the U(VI) reduction Rate.
Bigeleisen, J., 1996. Nuclear size and Shape Effects in Chemical Reactions. Isotope Chemistry of the Heavy elements. J. Am. Chem. Soc. 118, 3676–3680.
Böning, P., Brumsack, H.-J., Böttcher, M.E., Schnetger, B., Kriete, C., Kallmeyer, J., Borchers, S.L., 2004. Geochemistry of Peruvian near-surface sediments. Geochim. Cosmochim. Acta 68, 4429–4451.
Brennecka, G., Wasylenki, L.E., Bargar, J.R., Weyer, S., Anbar, A.D., 2011. Uranium isotope fractionation during adsorption to Mn-oxyhydroxides. Environ. Sci. Technol. 45, 1370–1375.
Brockmann, C., Fahrbach, E., Huyer, A., Smith, R.L., 1980. The poleward undercurrent along the Peru coast: 5 to 15 ° S. Deep. Res. 27A, 847–856.
Bruggmann, S., Scholz, F., Klaebe, R.M., Canfield, D.E., Frei, R., 2019. Chromium isotope cycling in the water column and sediments of the Peruvian continental margin. Geochim. Cosmochim. Acta 257, 224–242.
Chase, Z., Anderson, R.F., Fleisher, M., 2001. Evidence from authigenic uranium for increased productivity of the glacial Subantarctic Ocean. Paleoceanography 16, 1–11.
Chen, J.H., Lawrence, Edwards R., Wasserburg, G.J., 1986. 238U,234U and232Th in seawater. Earth Planet. Sci. Lett. 80, 241–251.
Chen, X., Romaniello, S.J., Herrmann, A.D., Wasylenki, L.E., Anbar, A.D., 2016. Uranium isotope fractionation during coprecipitation with aragonite and calcite. Geochim. Cosmochim. Acta 188, 189–207.
Chen, X., Romaniello, S.J., Herrmann, A.D., Hardisty, D., Gill, B.C., Anbar, A.D., 2018a. Diagenetic effects on uranium isotope fractionation in carbonate sediments from the Bahamas. Geochim. Cosmochim. Acta 237, 294–311.
Chen, X., Romaniello, S.J., Herrmann, A.D., Samankassou, E., Anbar, A.D., 2018b. Biological effects on uranium isotope fractionation (238U/235U) in primary biogenic carbonates. Geochim. Cosmochim. Acta 240, 1–10.
Chen, X., Zheng, W., Anbar, A.D., 2020. Uranium Isotope Fractionation (238U/235U) during U(VI) Uptake by Freshwater Plankton. Environ. Sci. Technol. 54, 2744–2752.
Chen, X., Romaniello, S.J., McCormick, M., Sherry, A., Havig, J.R., Zheng, W., Anbar, A. D., 2021. Anoxic depositional overprinting of 238U/235U in calcite: when do carbonates tell black shale tales? Geology 49, 1193–1197.
Clark, S.K., Johnson, T.M., 2008. Effective isotopic fractionation factors for solute removal by reactive sediments: a laboratory. Environ. Sci. Technol. 42, 7850–7855.
Cole, D.B., Planavsky, N.J., Longley, M., Böning, P., Wilkes, D., Wang, X., Swanner, E.D., Wittkop, C., Loydell, D.K., Busigny, V., Knudsen, A.C., Sperling, E.A., 2020. Uranium isotope fractionation in non-sulfidic anoxic settings and the global uranium isotope mass balance. Glob. Biogeochem. Cycles 34, 1–22.
Dale, A.W., Sommer, S., Lomnitz, U., Montes, I., 2015. Organic carbon production, mineralisation and preservation on the. Biogeosciences 12.
Diamond, C.W., Lyons, T.W., 2018. Mid-Proterozoic Redox Evolution and the Possibility of Transient Oxygenation Events, pp. 1–11.
Dunk, R.M., Mills, R.A., Jenkins, W.J., 2002. A reevaluation of the oceanic uranium budget for the Holocene. Chem. Geol. 190, 45–67.
Endrizzi, F., Rao, L., 2014. Chemical speciation of uranium(VI) in marine environments: Complexation of calcium and magnesium ions with [(UO2)(CO3)3]4-and the effect on the extraction of uranium from seawater. Chem. - A Eur. J. 20, 14499–14506.
Eroglu, S., Scholz, F., Frank, M., Siebert, C., 2020. Influence of particulate versus diffusive molybdenum supply mechanisms on the molybdenum isotope composition of continental margin sediments. Geochim. Cosmochim. Acta 273, 51–69.
Francois, R., Bacon, M.P., Altabet, M.A., Labeyrie, L.D., 1993. Glacial Interglacial changes in sediment rain rate in the SW Indian sector of sub-Antarctic water as recorded by 230Th, 231Pa, U, and d15N. Paleoceanography 8, 611–629.
Froelich, P.N., Arthur, M.A., Burnett, W.C., Deakin, M., Hensley, V., Jahnke, R., Kaul, L., Kim, K.H., Roe, K., Soutar, A., Vathakanon, C., 1988. Early diagenesis of organic matter in Peru continental margin sediments: Phosphorite precipitation. Mar. Geol. 80, 309–343.
Fujii, Y., Higuchi, N., Haruno, Y., Nomura, M., Suzuki, T., 2006. Temperature dependence of isotope effects in uranium chemical exchange reactions. J. Nucl. Sci. Technol. 43, 400–406.
Glenn, C.R., Arthur, M.A., 1988. Petrology and major element geochemistry of Peru margin phosphorites and associated diagenetic minerals: Authigenesis in modern organic-rich sediments. Mar. Geol. 80, 231–267.
Goto, K.T., Anbar, A.D., Gordon, G.W., Romaniello, S.J., Shimoda, G., Takaya, Y., Tokumaru, A., Nozaki, T., Suzuki, K., Machida, S., Hanyu, T., Usui, A., 2014. Uranium isotope systematics of ferromanganese crusts in the Pacific Ocean: Implications for the marine 238U/235U isotope system. Geochim. Cosmochim. Acta 146, 43–58.
Gutiérrez, D., Enríquez, E., Purca, S., Quipúzcoa, L., Marquina, R., Flores, G., Graco, M., 2008. Oxygenation episodes on the continental shelf of Central Peru: Remote forcing and benthic ecosystem response. Prog. Oceanogr. 79, 177–189.
Hayes, C.T., Martínez-García, A., Hasenfratz, A.P., Jaccard, S.L., Hodell, D.A., Sigman, D. M., Haug, G.H., Anderson, R.F., 2014. A stagnation event in the deep South Atlantic during the last interglacial period. Science (80-.) 346, 1514–1517.
Henderson, G.M., 2002. Seawater (234U/238U) during the last 800 thousand years. Earth Planet. Sci. Lett. 199, 97–110.
Hinojosa, J.L., Stirling, C.H., Reid, M.R., Moy, C.M., Wilson, G.S., 2016. Trace metal cycling and 238U/235U in New Zealand's fjords: Implications for reconstructing global paleoredox conditions in organic-rich sediments. Geochim. Cosmochim. Acta 179, 89–109.

Holmden, C., Amini, M., Francois, R., 2015. Uranium isotope fractionation in Saanich Inlet: A modern analog study of a paleoredox tracer. Geochim. Cosmochim. Acta 153, 202–215.
Huerta-Diaz, M.A., Morse, J.W., 1990. A quantitative method for determination of trace metal concentrations in sedimentary pyrite. Mar. Chem. 29, 119–144.
Keeling, R.F., Körtzinger, A., Gruber, N., 2010. Ocean Deoxygenation in a Warming World. Annu. Rev. Mar. Sci. 2, 199–229.
Kigoshi, K., 1971. Alpha recoil thorium-234: dissolution into water and uranium-234/uranium-238 disequilibrium in nature. Science (80-.) 173, 47–48.
Klinkhammer, G.P., Palmer, M.R., 1991. Uranium in the oceans: where it goes and why. Geochim. Cosmochim. Acta 55, 1799–1806.
Krissek, L.A., Scheidegger, K.F., Kulm, L.D., 1980. Surface sediments of the Peru-Chile continental margin and the Nazca plate. Geol. Soc. Am. Bull. 91, 321–331.
Ku, T.L., Knauss, K.G., Mathieu, G.G., 1977. Uranium in open ocean: concentration and isotopic composition. Deep. Res. 24, 1005–1017.
Kumar, N., Anderson, R.F., Mortlock, R.A., Froelich, P.N., Kubib, P., Dittrich-Hannen, B., Suter, M., 1995. Increased biological productivity and export production in the glacial Southern Ocean. Nature 378, 675–680.
Langmuir, D., 1978. Uranium solution-mineral equilibria at low temperatures with applications to sedimentary ore deposits. Geochim. Cosmochim. Acta 42, 547–569.
Lau, K.V., Romaniello, S.J., Zhang, F., 2019. Earth System Science the Uranium Isotope Paleoredox Proxy. Cambridge University Press.
Lau, K.V., Lyons, T.W., Maher, K., 2020. Uranium reduction and isotopic fractionation in reducing sediments: Insights from reactive transport modeling. Geochim. Cosmochim. Acta 287, 65–92.
Levin, L., Gutiérrez, D., Rathburn, A., Neira, C., Sellanes, J., Muñoz, P., Gallardo, V., Salamanca, M., 2002. Benthic processes on the Peru margin: A transect across the oxygen minimum zone during the 1997-98 El Niño. Prog. Oceanogr. 53, 1–27.
Lovely, D.R., Phillips, J.P., Gorby, Y.A., Landa, E.R., 1991. Microbial reduction of uranium. Nature 350, 413–416.
McManus, J., Berelson, W.M., Klinkhammer, G.P., Hammond, D.E., Holm, C., 2005. Authigenic uranium: Relationship to oxygen penetration depth and organic carbon rain. Geochim. Cosmochim. Acta 69, 95–108.
McManus, J., Berelson, W.M., Severmann, S., Poulson, R.L., Hammond, D.E., Klinkhammer, G.P., Holm, C., 2006. Molybdenum and uranium geochemistry in continental margin sediments: Paleoproxy potential. Geochim. Cosmochim. Acta 70, 4643–4662.
Moffett, J.W., German, C.R., 2018. The U.S. GEOTRACES Eastern Tropical Pacific Transect (GP16). Mar. Chem. 201, 1–5.
Molina-Cruz, A., 1977. The relation of the southern trade winds to upwelling processes during the last 75,000 years. Quat. Res. 8, 324–338.
Morford, J.L., Martin, W.R., Carney, C.M., 2009. Uranium diagenesis in sediments underlying bottom waters with high oxygen content. Geochim. Cosmochim. Acta 73, 2920–2937.
Noordmann, J., Weyer, S., Montoya-pino, C., Dellwig, O., Neubert, N., Eckert, S., 2015. Uranium and molybdenum isotope systematics in modern euxinic basins : Case studies from the Central Baltic Sea and the Kyllaren fjord (Norway). Chem. Geol. 396, 182–195.
Phan, T.T., Gardiner, J.B., Capo, R.C., Stewart, B.W., 2018. Geochemical and multi-isotopic (87Sr/86Sr, 143Nd/144Nd, 238U/235U) perspectives of sediment sources, depositional conditions, and diagenesis of the Marcellus Shale, Appalachian Basin, USA. Geochim. Cosmochim. Acta 222, 187–211.
Rademacher, L.K., Lundstrom, C.C., Johnson, T.M., Sanford, R.A., Zhao, J., Zhang, Z., 2006. Experimentally determined uranium isotope fractionation during reduction of hexavalent U by bacteria and zero valent iron. Environ. Sci. Technol. 15, 6943–6948.
Reimers, C., Suess, E., 1983. In: Spatial and temporal patterns of organic matter accumulation on the Peru continental margin, Suess, E., Thiede, J. (Eds.), Coastal Upwelling: Part B. Sedimentary Record of Ancient Coastal Upwelling. Plenum Press, New York, pp. 331–346.
Rolison John, M., Stirling, C.H., Middag, R., Rijkenberg, M.J.A., 2017. Uranium stable isotope fractionation in the Black Sea: Modern calibration of the 238 U/235 U paleo-redox proxy. Geochim. Cosmochim. Acta 203, 69–88.
Romaniello, S.J., 2012. Incorporation of Preservation of Molybdenum and Uranium Isotope Variations in Modern Marine Sediments. University of Arizona.
Romaniello, S.J., Herrmann, A.D., Anbar, A.D., 2013. Uranium concentrations and 238U/235U isotope ratios in modern carbonates from the Bahamas: Assessing a novel paleoredox proxy. Chem. Geol. 362, 305–316.
Salvatteci, R., Gutiérrez, D., Field, D., Sifeddine, A., Ortlieb, L., Bouloubassi, I., Boussafir, M., Ird, U.M.R., Pierre, I., Laplace, S., Cedex, B., Imarpe, P., General, D., Oceanográficas, D.I., 2014. The response of the Peruvian Upwelling Ecosystem to centennial-scale global change during the last two millennia. Clim. Past 10, 715–731.
Schauble, E., 2007. Role of nuclear volume in driving equilibrium stable isotope fractionation of mercury, thallium, and other very heavy elements. Geochim. Cosmochim. Acta 71, 2170–2189.
Schlitzer, R., Anderson, R.F., Masferrer, E., Lohan, M., Daniels, C., Dehairs, F., Deng, F., Thi, H., Duggan, B., 2018. The GEOTRACES intermediate data product 2017. Chem. Geol. 493, 210–223. https://doi.org/10.1016/j.chemgeo.2018.05.040.
Schmidtko, S., Stramma, L., Visbeck, M., 2017. Decline in global oceanic oxygen content during the past five decades. Nature 542, 335–339.
Scholz, F., 2018. Identifying oxygen minimum zone-type biogeochemical cycling in Earth history using inorganic geochemical proxies. Earth Sci. Rev. 184, 29–45.
Scholz, F., Hensen, C., Noffke, A., Rohde, A., Liebetrau, V., Wallmann, K., 2011. Early diagenesis of redox-sensitive trace metals in the Peru upwelling area – response to ENSO-related oxygen fluctuations in the water column. Geochim. Cosmochim. Acta 3 (75), 7257–7276.
Scholz, F., Siebert, C., Dale, A.W., Frank, M., 2017. Intense molybdenum accumulation in sediments underneath a nitrogenous water column and implications for the reconstruction of paleo-redox conditions based on molybdenum isotopes. Geochim. Cosmochim. Acta 213, 400–417.
Severmann, S., Thomson, J., 1998. Investigation of the ingrowth of radioactive daughters of in Mediterranean sapropels as a potential dating tool. Chem. Geol. 50, 317–330.
Stetten, L., Mangeret, A., Brest, J., Seder-Colomina, M., Le Pape, P., Ikogou, M., Zeyen, N., Thouvenot, A., Julien, A., Alcalde, G., Reyss, J.L., Bombled, B., Rabouille, C., Olivi, L., Proux, O., Cazala, C., Morin, G., 2018. Geochemical control on the reduction of U(VI) to mononuclear U(IV) species in lacustrine sediments. Geochim. Cosmochim. Acta 222, 171–186.
Stirling, C.H., Andersen, M.B., Potter, E.K., Halliday, A.N., 2007. Low-temperature isotopic fractionation of uranium. Earth Planet. Sci. Lett. 264, 208–225.
Stirling, C.H., Andersen, M.B., Warthmann, R., Halliday, A.N., 2015. Isotope fractionation of 238U and 235U during biologically-mediated uranium reduction. Geochim. Cosmochim. Acta 163, 200–218.
Stylo, M., Neubert, N., Wang, Y., Monga, N., Romaniello, S.J., Weyer, S., Bernier-Latmani, R., 2015. Uranium isotopes fingerprint biotic reduction. Proc. Natl. Acad. Sci. U. S. A. 112, 5619–5624.
Thamdrup, B., Dalsgaard, T., Peter, N., 2012. Deep-Sea Research I Widespread functional anoxia in the oxygen minimum zone of the Eastern South Pacific. Deep. Res. Part I 65, 36–45.
Tissot, L.H., Dauphas, N., 2015. Uranium isotopic compositions of the crust and ocean: Age corrections, U budget and global extent of modern anoxia. Geochim. Cosmochim. Acta 167, 113–143.
Tribovillard, N., Algeo, T.J., Lyons, T., Riboulleau, A., 2006. Trace metals as paleoredox and paleoproductivity proxies: an update. Chem. Geol. 232, 12–32.
Wang, X., Planavsky, N.J., Reinhard, C.T., Hein, J.R., Johnson, T.M., 2016. A cenozoic seawater redox record derived from 238U/235U in ferromanganese crusts. Am. J. Sci. 316, 64–83.
Weyer, S., Anbar, A.D., Gerdes, A., Gordon, G.W., Algeo, T.J., Boyle, E.A., 2008. Natural fractionation of 238U/235U. Geochim. Cosmochim. Acta 72, 345–359.
Zhang, F., Xiao, S., Kendall, B., Romaniello, S.J., Cui, H., Meyer, M., Gilleaudeau, G.J., Kaufman, A.J., Anbar, A.D., 2018. Extensive marine anoxia during the terminal Ediacaran Period. Sci. Adv. 4, 1–12.
Zheng, Y., Andersen, R.F., van Geen, A., Fleisher, M.Q., 2002a. Remobilization of authigenic uranium in marine sediments by bioturbation. Geochim. Cosmochim. Acta 66, 1759–1772.
Zheng, Y., Anderson, R.F., van Geen, A., Fleisher, M.Q., 2002b. Preservation of particulate non-lithogenic uranium in marine sediments. Geochim. Cosmochim. Acta 66, 3085–3092.